Available online at www.sciencedirect.com

SciVerse ScienceDirect

Energy Procedia 29 (2012) 181 – 191

Energy Procedia

World Hydrogen Energy Conference 2012

New catalysts based on Ni-Birnessite and Ni-Todorokite for the efficient production of hydrogen by bioethanol steam reforming

A. Fuertes[a], J.F. Da Costa-Serra[a], A. Chica[a,*]

[a]*Instituto de Tecnolgía Química (UPV-CSIC), Universidad Politécnica de Valencia, Consejo Superior de Investigaciones Científicas, Avenida de los naranjos s/n, Valencia 46022, Spain*

Abstract

Catalytic steam reforming of bioethanol seems to be a promise option to produce renewable hydrogen; however efficient catalysts are still under development. Recently, manganese oxide based materials (MO) are the subject of intense research as low cost, efficient, and environmentally friendly catalysts. Among them MO with layer and tunnel structure have received significant attention due to their excellent catalytic activity. Specifically, we have explored the catalytic performance of two MO containing Ni (Birnessite and Todorokite). We find that both materials are highly active and selective to produce hydrogen by steam reforming of bioethanol. Their characterization by DRX, BET area, TPR, and TEM, has allowed to find that the excellent performance exhibited by these materials could be attributed to the especial structure of these MO, which would provide high-quality positions for the stabilization of the Ni metal particles.

Keywords: Bioethanol, Steam Reforming, Hydrogen, Todorokite, Biernessite, Nickel.

1. Introduction

Hydrogen is identified as a very promising renewable energy source to satisfy energy needs while protecting the environment [1]. Unfortunately, it is not freely available in nature and it must be produced by some means. About 95% of the hydrogen we use today comes from natural gas reforming. But to realize the full benefits of a hydrogen economy-sustainability, increased energy security, diverse energy

* Corresponding author. Tel.: +34 963 87 70 00-78508; fax: +34 963 87 78 09.
E-mail address: achica@itq.upv.es

doi:10.1016/j.egypro.2012.09.023

supply and reduced air pollution hydrogen must be produced cleanly, efficiently, and affordably from available renewable resources. Hydrogen can be produced from biomass, a renewable and CO_2-neutral energy source with respect to the green house effect [2-5]. Because biomass consumes atmospheric carbon dioxide (CO_2) during growth, it can have a small net CO_2 impact compared with fossil fuels.

Reforming of renewable biomass feedstocks [6], such as bio-ethanol, has become an increasingly important and active research area in view of hydrogen production [2,7-11]. In comparison with other fuels, bio-ethanol presents a series of advantages, since they are easier to store, handle and transport in a safe way due to is lower toxicity and volatility. In addition, from the environmental point of view, bio-ethanol presents important advantages since it is metal-free and does not release pollutant gases (SO_x, NO_x and others) [12,13]. Numerous studies have been focused on the design, development, and optimization of catalytic materials for ethanol steam reforming. Nevertheless, efficient catalysts for bioethanol steam reforming are still under development. Several reviews about the development of catalysts applied to ethanol steam reforming have been published lately [7,10,11,14]. Catalytic materials such as transition metals supported on oxides and precious metals supported on oxides are reported in these reviews. Among them, Ni-based catalysts are widely accepted due to their appropriate low-cost compared to precious metals. For the steam reforming of ethanol Ni has exhibited good performance by favoring C-C bond and O-H bond rupture [15]. In general, the catalytic performance of each catalyst (activity, selectivity and stability) will depend on the nature of metal, type of precursor, preparation method, type of support, presence of additives, and operating conditions. Among them, it is found that support plays an important role in the preparation of highly active and selective bioethanol steam reforming catalysts since it helps in the dispersion of metal catalyst and enhances its activity via metal-support interactions. In addition, synthesized methods and pretreatment conditions over supported nickel catalysts are also important issues to prepared highly active steam reforming catalysts. This way, the activity of the steam reforming catalyst can be improved achieving a good dispersion of metallic sites on the support, while coke formation could decrease using non-acidic supports that would avoid the ethanol dehydration reaction [16-20].

Thus, it is clear that the chemical composition, textural properties of the support and synthesis method play important roles in the preparation of highly active steam reforming catalyst since they can improve the dispersion of metal catalysts [12] and avoid their sinterization [21]. Recently, manganese oxide based materials (MO) are the subject of intense research as low cost, efficient, and environmentally friendly catalysts [22,23]. Among them MO with layer and tunnel structure have received significant attention due to their excellent catalytic activity [24-26]. Thus, we presented here the results obtained in the bioethanol steam reforming using Ni metallic particles incorporated on two of these manganese oxide materials, particularly on Birnesite and Todorokite structures. The characterization of these Ni-promoted catalysts based on the OM has been completed and connected to their catalytic performance.

2. Experimental

2.1. Preparation of catalysts

The synthesis of Ni-Birnessite and Ni-Todorokite was carried out according to Onda et al. [27].

The chemicals were purchased from Sigma-Aldrich. To prepared the Ni-Birnessite a solution A containing $Ni(NO_3)_2$ $6H_2O$ (1.87 g) and $MnCl_2$ $4H_2O$ (6.37 g) in 100 mL of Milli-Q water was added dropwise over a period of 10 min at room temperature (298 K) into a solution B formed by $KMnO_4$ (2.02 g) and NaOH (36 g) in 100 mL of Milli-Q water. After the solutions were mixed, they were stirred for a total of 30 min. The suspension was aged at room temperature for 24 h, and it was filtered and washed

with Milli-Q water until the pH was about 7. The resultant material was a layered birnessite material, referred to as Ni-BIR.

Ni-Todorokite was prepared using the before Ni-Birnessite. It was ion-exchanged with 200 mL of a 0.1 mol/L $Ni(NO_3)_26H_2O$ aqueous solution at room temperature for 24 h. The resultant layered sample was washed and filtered ten times with 200 mL of Milli-Q water. Finally, it was treated under hydrothermal conditions (433 K for 48 h in an autoclave lined with Teflon) and the resultant solid was washed and filtered with Milli-Q water, and dried at 333 K to yield Ni-TOD.

2.2. Characterization techniques

The nickel content in the samples was determined by atomic absorption spectrophotometry (AAS) in a Varian Spectra A-l0 Plus apparatus.

Textural properties of the Ni-Birnessite and Ni-Todorolite materials were obtained from the nitrogen adsorption isotherms determined at 77 K in a Micromeritics ASAP 2000 equipment. Surface areas were calculated by the BET method and the pore-size distributions were obtained using the BJH formalism. Prior to the adsorption measurements the samples were outgassed at 473 K for 24 h.

X-ray diffraction was used to identify the nature of the crystalline manganese and nickel oxides and metallic nickel phases. XRD patterns were obtained at room temperature in a Philips X'pert diffractometer using monochromatized CuKα radiation.

The reduction behavior of the supported oxidized nickel phases was studied by temperature-programmed reduction (TPR) in a Micromeritics Autochem 2910 equipment. The H_2 consumption rate was monitored in a thermal conductivity detector (TCD) previously calibrated using the reduction of CuO as reference.

The amount of carbon deposited in the catalysts after steam reforming reaction was determined by elemental analysis using a Carlo Erba 1106 analyzer.

2.3. Catalytic study

Steam reforming experiments were carried out in a continuous fixed bed reactor at atmospheric pressure, H_2O/EtOH molar ratio of 13, GHSV 4700 h^{-1} and a range of temperatures between 673 K and 873 K. Before reaction the catalysts were reduced "in situ" in flow of H_2 (1.67 cm^3s^{-1}) at 873 K for 2 h.

In a typical catalytic test the reactor was loaded with 0.3 ml of catalyst, ~0.15 g, (grain-size: 0.25-0.42 mm), diluted with 3 g of carborundum (SiC) (grain-size: 0.60-0.80 mm), The water/ ethanol mixture was fed from a pressurized container using a liquid flow controller (Bronkhorst), and vaporized at 473 K into a stream of nitrogen. The total gas flow was 2 cm^3s^{-1} (83.7 vol% N_2).

The analysis of the compounds of reaction was carried out online using a gas chromatograph (Varian 3800) equipped with two columns (TRB-5, L = 30 m, DI = 0.25 mm; CarboSieve SII, L = 3 m, DI = 2.1 mm) and two detectors, a thermal conductivity and flame ionization (FID).

The bioethanol conversion and selectivity to the different reaction products were determined according to the Eqs. (1) and (2), where $(F_{EtOH})_O$ is the flow of ethanol fed to the reactor (mol s-1), $(F_{EtOH})_f$ the flow of ethanol that comes from the reactor and F_j the flow of product j that comes from the reactor. Selectivity values were calculated as the molar percentage of the products obtained, excluding water.

$$\text{Conv. (\%, mol)} = \frac{(F_{EtOH})_o - (F_{EtOH})_f}{(F_{EtOH})_o} \times 100 \qquad (1)$$

$$\text{Selec. (\%, mol)} = \frac{F_j}{(\Sigma F_j)_{products}} \times 100 \qquad (2)$$

3. Results and discussion

3.1. Characterization

X-ray diffraction patterns of synthesized Ni-BIR and Ni-TOD materials are showed in Figure 1. As it can be seen all the diffraction peaks can be attributed to the Birnessite and Todorokite phases [27], suggesting that Ni-BIR and Ni-TOD has been correctly synthesized.

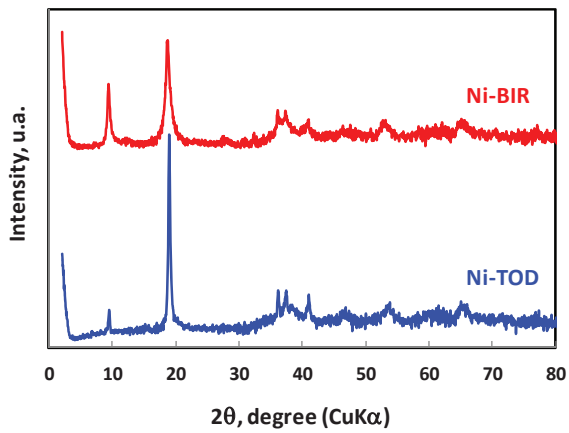

Fig. 1. XRD patterns of N-BIR and Ni-TOD as they were synthesized.

SEM images of Ni-BIR and Ni-TOD are shown in Figure 2. Both materials contain sheet-shaped crystallites. This morphology seems to be reflected in the XRD where the high intensity of the XRD-main peaks would indicate growth direction of birnessite and todorokite.

Specific area of Ni-BIR and Ni-TOD was also determined and it was found similar in both materials (18 and 16 m^2/g, respectively), Table 1.

XRD, SEM and specific area data suggest that both materials are comparable in crystallinity, morphology and crystalline size.

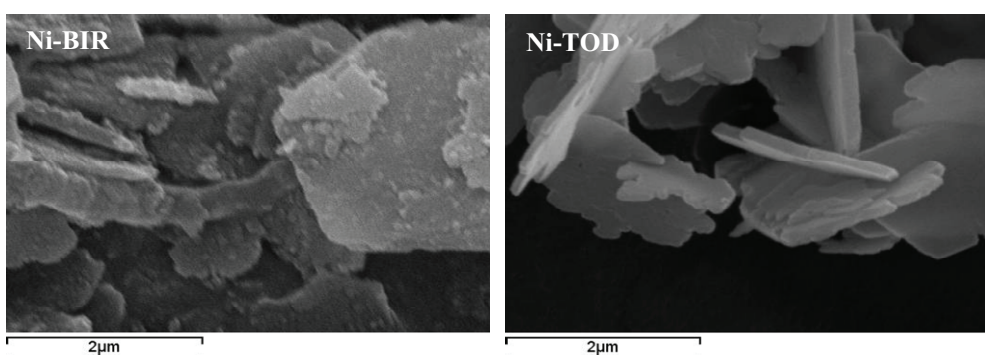

Fig. 2. SEM micrograhs of Ni-BIR and Ni-TOD samples.

Ni-BIR and Ni-TOD were calcined at 873 K and reduced at 873 K before reaction. Figure 3 shows the XRD of the calcined samples. As it can be seen calcined materials shows similar XRD pattern with diffraction peaks corresponding to manganese oxides and NiO phases (JCPDS Nº: 22 1189).

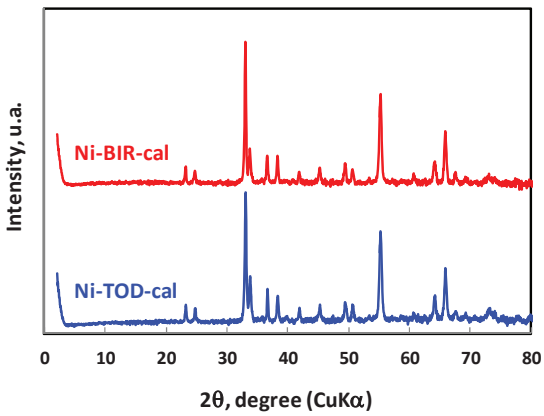

Fig. 3. XRD patterns of Ni-BIR and Ni-TOD after calcination at 873 K.

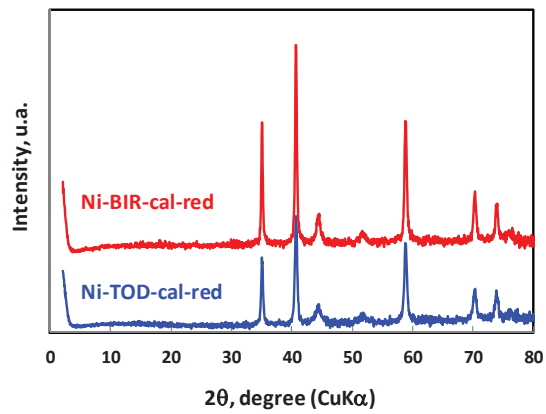

Fig. 4. XRD patterns of Ni-BIR and Ni-TOD after calcination at 873 K and reduction at 873 K.

After reduction with hydrogen at 873 K, the peaks corresponding to NiO disappear and appear those due to the reduced metallic nickel phases, Figure 4. The manganese oxide phases also changes to more reduces forms but metallic manganese phases were not detected. Crystallite size of Ni metallic particles was determined using the Scherrer equation from the corresponding characteristic peaks of each phase [28]. It can be seen in Table 1 that metallic Ni particles present on Ni-TOD are significantly lower than that in Ni-BIR. Particle size of the metallic Ni was also determined by TEM in order to corroborate the Ni metallic particle size calculated by XRD. As it can be seen in Table 1 and Figure 5, the particle size matched quite well with those obtained by XRD. The lower Ni metallic particle size detected over the Ni-TOD could be related to its particular morphology and crystalline structure. It is possible that the crystalline structure of this material can help to provide high-quality positions for the accommodation and stabilization of Ni metallic particles during the calcination and reduction steps. On the contrary, the Birnessite structure seems to lead to higher sinterization of Ni during the calcination and reduction steps, leading to higher metallic particle size.

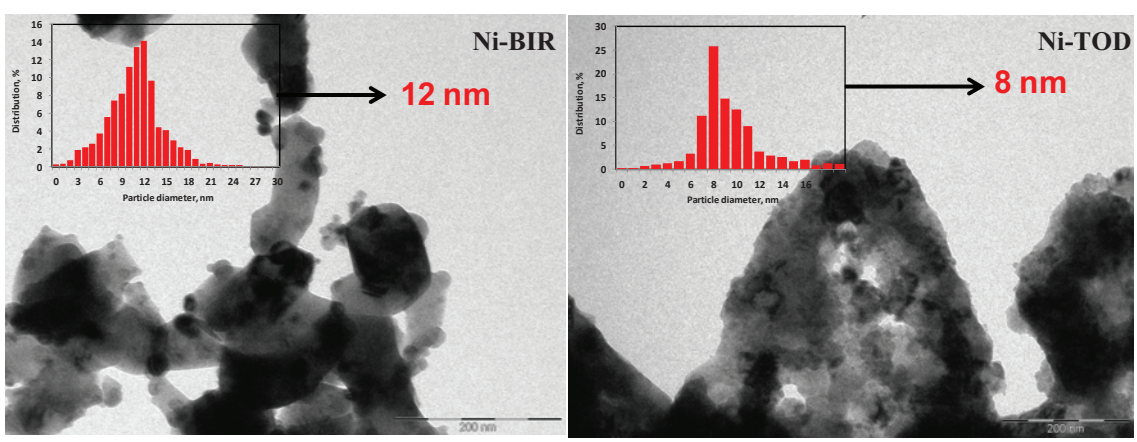

Fig. 5. TEM micrographs of the Ni-BIR and Ni-TOD after calcination and reduction at 873 K.

Table 1. Ni content and textural properties of OM materials promoted with Ni. Particle size of metallic Ni particles determined by XRD and TEM.

Catalyst	Ni content (wt.%)	BET surface area (m^2/g^{-1})	Metallic Ni Particle size (nm)	
			XRD	TEM
Ni-BIR	13.4	18	15	12
Ni-TOD	15.6	16	9	8

The reduction behaviors of the nickel oxide particles present in these materials have been studied by temperature programmed reduction (TPR). The corresponding reduction curves are show in Figure 6. As observed, both materials present two main reduction features in a range between 580 K and 650 K, which correspond to the two-step reduction process of NiO. The first one at lower temperature around 580-620 K, it can be assigned to the reduction of Ni^{2+} with weak interaction with the support [29-32]. The second one at 620-650 K, can be attributed to a strong Ni-support interaction [29,32]. The differences found in the temperature reduction for the Ni-BIR and Ni-TOD could be related to the Ni metallic particle sizes determined by XRD or TEM (Table 1). Thus, smallest Ni particle size (over Todorokite) shows the highest reduction temperature for its corresponding second peak, and consequently, the strongest Ni supports interactions.

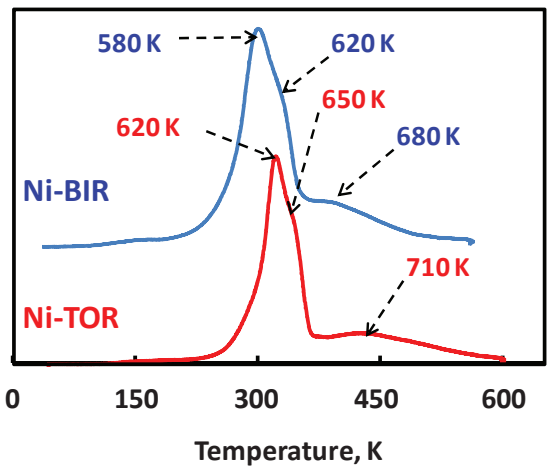

Fig. 6. TPR profiles of Ni-BIR and Ni-TOD.

Additional small hydrogen consumption about of 680 K and 710 K has been also observed for both samples (Ni-BIR and Ni-TOD, respectively). This reduction peak could be ascribed to the reduction of nickel oxide in a high interaction with the support.

The reduction temperature and the peak width are indications of the degree of reduction and the level of interaction between different species, respectively. High reduction temperature indicates difficulty in reduction whereas broad peaks indicate a high degree of interaction between the species and the support [33]. TPR results seem to indicate that nickel oxides exhibit higher interaction with Todorokite material, since the two main peaks appear at 620 K and 650 K while for the Ni-BIR the peaks shift at lower reduction temperatures (580 K and 620 K, respectively). These differences in the reduction temperature could be related to the different size of the Ni metallic particles found for each support (Table 1). Smaller particle size would favor the appearance of stronger metal-support interactions, increasing the reduction temperature. Indeed, the highest reduction temperatures were detected for the Ni-TOD sample, which exactly showed the smallest Ni metallic particle sizes.

3.2. Catalytic activity

Figure 7 shows the conversion of bioethanol with the reaction temperature. As it can be seen both materials present a very high activity in comparison with reference materials based on zinc oxide promoted with Ni and Co, which have been described in literature as excellent catalysts for the steam

reforming of ethanol [34,35]. In terms of activity, it cannot be found differences between Ni-BIR and Ni-TOD since the bioethanol conversion is complete in all the reaction temperature range here studied (673-873 K). Analogously, the selectivity to hydrogen is very high in both catalysts, but in this case the differences with the reference materials are lower, Figure 8. This result shows the positive effect that these materials based on manganese oxides has as precursor of reforming catalysts in the steam reforming of bioethanol.

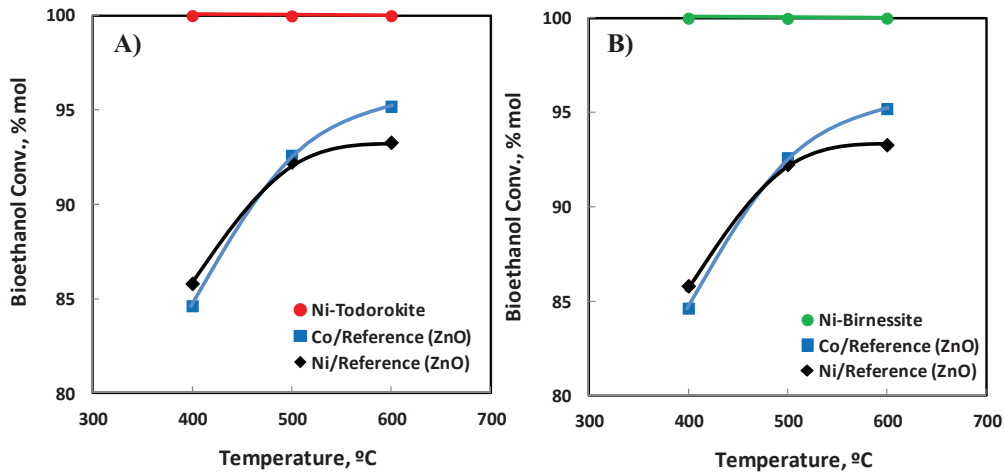

Fig. 7. Conversion of bioethanol versus reaction temperature. A) Ni-BIR and B) Ni-TOD. Reaction conditions: H_2O/bioEtOH=13, GHSV= 4700 h^{-1} and atmospheric pressure.

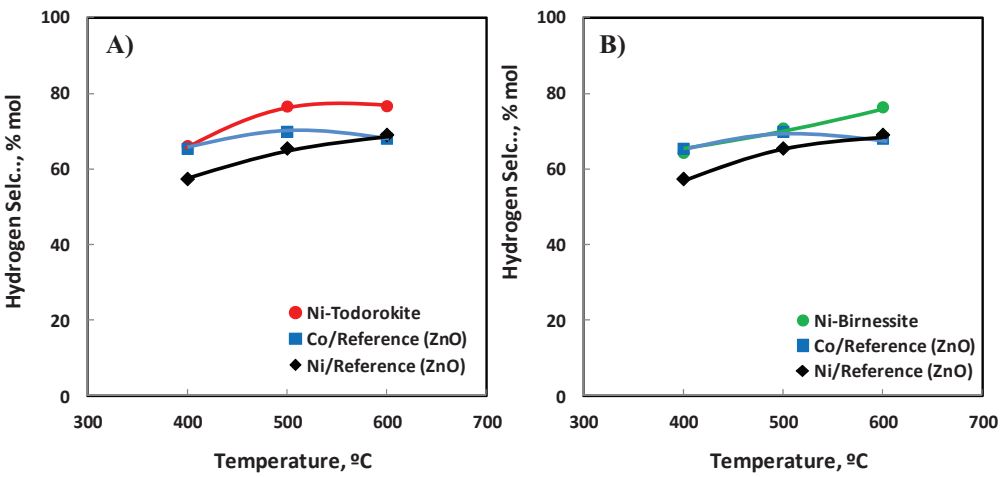

Fig. 8. Hydrogen selectivity version reaction temperature. A) Ni-BIR and B) Ni-TOD. Reaction conditions: H_2O/bioEtOH=13, GHSV= 4700 h^{-1} and atmospheric pressure.

Catalytic activity of the Ni-BIR and Ni-TOD materials was also studies with the reaction time. After 24 hours of reaction at 773 K (Table 2) it can be seen that Ni-BIR and Ni-TOD present a low deactivation over time. It is well known that the stability of a reforming catalyst is strongly influenced by the coke deposition and metal sintering [24]. After reaction, the catalysts showed black color, it is an indicator of coke deposition. The elemental analysis of the catalysts after the reaction shows that the deposited coke

was greater in the case of Ni-TOD (Table 2), however, deactivation was similar to the Ni-BIR and lower than in the reference materials, at least during the reaction time used in this catalytic study (24 hours). This result suggests that the lost of activity, in the Ni-TOD, could be related rather to the coke deposition

Table 2. Catalytic results for the bioethanol steam reforming on Ni-BIR and Ni-TOD. Bioethanol conversion values obtained at two reaction times, 5h and 24h. Products selectivity values obtained at 5 h of reaction time. Reaction conditions: H_2O/bioEtOH = 13, GHSV = 4700 h^{-1}, atmospheric pressure and 773 K.

	5 hour				24 hours	
	Conv. EtOH, % mol	**CH4**	**CO**	**C2H4**	**Conv. EtOH, % mol**	**Carbon, wt.%**
Ni-BIR	99.00	1.92	1.76	0.01	93.59	9.0
Ni-TOD	98.01	1.99	1.66	0.06	94.31	21.0
Ni-Reference (ZnO)	93.29	4.19	9.17	0.14	74.19	18.4
Co-Reference (ZnO)	94.00	3.78	5.85	0.12	83.78	9.8

instead of Ni sintering. In order to corroborate this hypothesis the used catalysts were studied by TEM. Figure 9 shows the TEM of the samples after reaction. Micrographs presented in Figure 9 show that the formation of coke deposit on the Ni-BIR is very low compared to the coke deposits detected on the Ni-TOD. On the contrary, the sinterization of the Ni metallic particles present in the used Ni-BIR is clearly higher that in Ni-TOD (from 12 nm to 39 nm and from 8nm to 17 nm, respectively). These results seem to confirm the before hypothesis in which the coke deposition was suggested as the main responsible of the deactivation detected in the Ni-Todorokite, while for Ni-BIR the deactivation would seem to be more related to the sinterization of the Ni metallic particles.

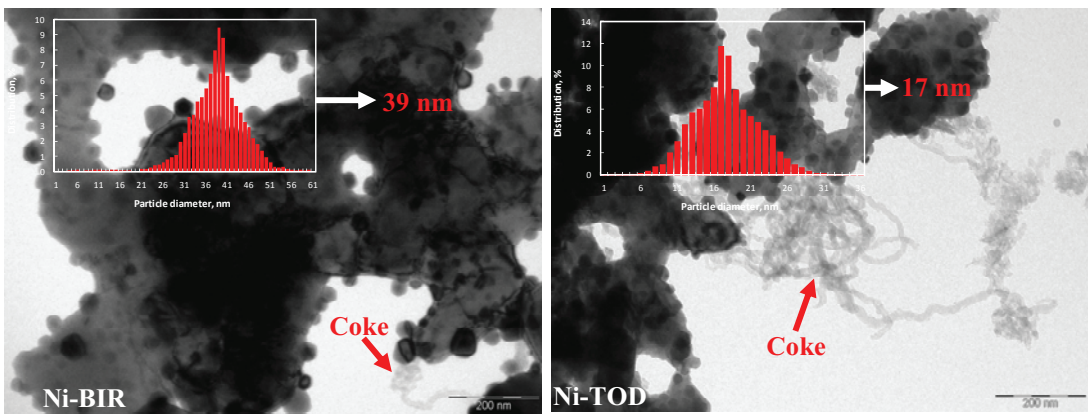

Fig. 9. TEM micrographs of the Ni-BIR and Ni-TOD after 24 h of reaction time.
Reaction conditions: H_2O/bioEtOH = 13, GHSV = 4700 h^{-1}, atmospheric pressure and 773 K.

Finally, it should be noted that Ni-BIR and Ni-TOD, not only showed high values of activity and selectivity in the production of hydrogen but also produced low concentrations of CO and CH_4 (Table 2).

All the results presented here show that it is possible to prepared new bioethanol steam reforming catalysts based on manganese oxides with structure type Birnessite and Todorokite and promoted with Ni with high activity, stability against coke deposition and able to reduce the formation of CO and CH_4.

4. Conclusions

We have prepared a new Ni promoted catalyst based on manganese oxides with structure type birnessite and todorokite with high activity, selectivity and resistant against coke deposition during the production of H_2 by steam reforming of bioethanol. Manganese oxide precursors seem to be the major responsible of the good performance of these catalysts. The results shown also that it is possible to produce "renewable" hydrogen with low concentrations of CH_4 and CO using these catalytic materials. It could lead to a significant benefit from the point of view of the direct use of this produced hydrogen.

Acknowledgements

The doctoral Javier Francisco Da Costa Serra acknowledges the CSIC for granted the scholarship predoctoral-JAE-CSIC.

References

[1] Zhang L, Li W, Liu J, Guo C, Wang Y, Zhang J. Ethanol steam reforming reactions over $Al_2O_3.SiO_2$-supported Ni–La catalysts. Fuel 2009;88:511–518.

[2] Ni M, Leung DYC, Leung MKH, Sumathy K. An overview of hydrogen production from biomass. Fuel Processing Technology 2006;87:461–472.

[3] Liguras DK, Kondarides DI, Verykios XE. Production of hydrogen for fuel cells by steam reforming of ethanol over supported noble metal catalysts. Appl Catal B: Environ 2003;43:345-354.

[4] Maggio G, Freni S, Cavallaro S. Light alcohols/methane fuelled molten carbonate fuel cells: a comparative study. J Power Sources 1998;74:17-23.

[5] Brown LF. A comparative study of fuels for on-board hydrogen production for fuel-cell-powered automobiles. Int J Hydrogen Energy 2001;26:381-397.

[6] Ma F, Hanna MA. Biodiesel production: a review. Bioresour Technol 1999;70:1-15.

[7] Ni M, Leung DYC,Leung MKH. A review on reforming bio-ethanol for hydrogen production. Int J Hydrogen Energy 2007;32:3238–3247.

[8] Huber GW, Iborra S, Corma A. Synthesis of transportation fuels from biomass: Chemistry, catalysts, and engineering. Chemical Review 2006;106:4044-4098.

[9] Duan S, Senkan S. Catalytic Conversion of Ethanol to Hydrogen Using Combinatorial Methods. Industrial & Engineering Chemistry Research 2005;44:6381–6386.

[10] Haryanto A, Fernando S, Murali N, Adhikari S. Current Status of Hydrogen Production Techniques by Steam Reforming of Ethanol: A Review. Energy & Fuels 2005;19:2098–2106.

[11] Vaidya PD, Rodrigues AE. Insight into steam reforming of ethanol to produce hydrogen for fuel cells. Chemical Engineering Journal 2006;117:39–49.

[12] Fierro V, Akdim O, Provendier H, Mirodatos C. Ethanol steam reforming over Ni-based catalysts. J Power Sources 2005;145:659–666.

[13] Comas J, Mariño F, Laborde M, Amadeo N. Bio-ethanol steam reforming on Ni/Al_2O_3 catalysts. Chem Eng J 2004;98:61–68.

[14] Ramirez de la Piscina P, Homs N. Use of biofuels to produce hydrogen (reformation processes). Chem. Soc. Rev. 2008; 37:2459-2467.

[15] Bellido JDA, Assaf EM. Appl. Catal. A 2009;352:179–187.

[16] Batista MS, Santos RKS, Assaf EM, Assaf JM, Ticianelli EA. Characterization of the activity and stability of supported cobalt catalysts for the steam reforming of ethanol. J Power Sources 2003;124:99–103.

[17] Cavallaro S, Mondello N, Freni S. Hydrogen produced from ethanol for internal reforming molten carbonate fuel cell. J Power Sources 2001;102:198–204.

[18] Llorca J, Piscina PR, Dalmon JA, Sales J, Homs N. CO-free hydrogen from steam reforming of bioethanol over ZnO-supported cobalt catalysts: effect of the metallic precursor. Appl Catal B Environ 2003;43:355–69.

[19] Llorca J, Homs N, Sales J, Fierro JL, Piscina PR. Effect of sodium addition on the performance of Co–ZnO-based catalysts for hydrogen production from bioethanol. J Catal 2004;222:470–80.

[20] Batista MS, Santos RKS, Assaf EM, Assaf JM, Ticinanelli EA. High efficiency steam reforming of ethanol by cobalt-based catalysts. J Power Sources 2004;134:27–32.

[21] Chica A, Sayas S. Effective and stable bioethanol steam reforming catalyst based on Ni and Co supported on all-silica delaminated ITQ-2 zeolite. Catal Today 2009;146:37-43.

[22] Suib SL. J. Mater. Chem. 2008;18:16323.

[23] Malinger KA, Ding YS, Sithambaram S, Espinal L, Gomez S, Suib SL. J. Catal. 2006;239:290.

[24] Sithambaram S, Kumar R, Son YC, Suib SL, J. Catal. 2008;253:269.

[25] Sithambaram S, Ding YS, Li WN, Shen XF, Suib SL, Green Chem. 2008;10:1029.

[26] Ghosh R, Shen XF, Villegas JC, Ding Y, Malinger K, Suib SL, J. Phys. Chem. B 2006;110:7592.

[27] Onda A, Hara S, Kajiyoshi D, Yanagisawa K. Appl. Catal. A: Gen. 2007;321:71-78.

[28] Cullity FD. Elements of X-Ray Diffraction. Addison-Wesley, London, 1878.

[29] B. Ernst, S. Libs, P. Chaumette, A. Kiennermann, Preparation and characterization of Fischer–Tropsch active Co/SiO_2 catalysts, Appl. Catal. A 186 (1999) 145-168.

[30] A.J. Vizcaíno, A. Carrero, J.A. Calles, Hydrogen production by ethanol steam reforming over Cu-Ni supported catalysts, Int. J. Hydrogen Energ. 32 (2007) 1450-1461.

[31] M.N. Barroso, M.F. Gomez, L.A. Arrúa, M.A. Abello, Hydrogen production by ethanol reforming over NiZnAl catalysts, Appl. Catal. A. Gen. 304 (2006) 116-123.

[32] K. Peng, L. Zhou, A. Hu, Y. Tang, D. Li, Synthesis and Magnetic Properties of Ni–SiO2 Nanocomposites, Mater. Chem. Phys. 111 (2008) 34-37.

[33] Akande AJ, Idem RO, Dalai AK. Synthesis, characterization and performance evaluation of Ni/Al2O3 catalysts for reforming of crude ethanol for hydrogen production. Appl Catal A:Gen 2005;287:159-175.

[34] Homs N, Llorca J, Ramírez de la Piscina P. Low-temperature steam-reforming of ethanol over ZnO-supported Ni and Cu catalysts - The effect of nickel and copper addition to ZnO supported cobalt-based catalysts. Catal Today 2006;116:361.

[35] Da Costa-Serra JF, Guil-López R, Chica A. Co/ZnO and Ni/ZnO catalysts for hydrogen production by bioethanol steam reforming. Influence of ZnO support morphology on the catalytic properties of Co and Ni phases. Inter J Hydrogen Energy 2010;13:6709-6716.